



REVIEW

Development of Perovskite Based Electrode Materials for Application in Electrochemical Supercapacitors: Present Status and Future Prospects

VINAYA JOSE^{1,*}, VISMAYA JOSE^{1,*}, C. FREEDA CHRISTY² and A. SAMSON NESARAJ^{1,*}

¹Department of Applied Chemistry, Karunya Institute of Technology and Sciences (Deemed to be University), Karunya Nagar, Coimbatore-641114, India

²Department of Civil Engineering, Karunya Institute of Technology and Sciences (Deemed to be University), Karunya Nagar, Coimbatore-641114, India

*Corresponding author: E-mail: drsamson@karunya.edu

Received: 26 September 2021;

Accepted: 1 December 2021;

Published online: 14 February 2022;

AJC-20678

Nanostructured electrode materials have illustrated predominant electrochemical properties in producing high-performance supercapacitors. Perovskite based nanostructures with formula ABO_3 have received broad consideration due to their excellent physical and chemical characteristics such as electrically active structure, electronic conductivity, ionic conductivity, supermagnetic, photocatalytic, thermoelectric, and dielectric properties, *etc.* Hence, perovskite based nano-structured materials are supposed to be promising, fascinating electrode materials for designing supercapacitors with high energy storage performance. In this review article, the recent progress and advances in designing perovskite based nanostructured electrode materials is discussed, which can provide as a guideline for the next generation of supercapacitor electrode design.

Keywords: Perovskite, Electrode materials, Electrochemical supercapacitors.

INTRODUCTION

The increasing energy demand needs researchers to explore new methods for designing electrode materials and evaluating their energy storage performances to create exceedingly progressed energy storage systems [1-6]. In energy storage frameworks, supercapacitor has received widespread consideration recently due to their good cycle stability, excellent power density and quick charge-discharge properties [7-10]. So far, supercapacitors have been used in combination with batteries to supply extra power required in numerous areas [11-13]. But they cannot be utilized in these applications as independent component, because of their energy density is lesser than that of batteries [14-17]. The scientific community is currently working to significantly progress the energy storage execution of supercapacitors through the production of new electrode materials and innovative device plan [18-21].

There are numerous electrode materials showing required characteristics, such as good cycle stability, high specific

capacitance and large rate capability [22-25]. In designing high performance supercapacitors, nanostructured electrode materials have outlined overwhelming electrochemical characteristics [26-29]. Nanostructuring of electrode materials may be an attainable strategy to significantly progress the electrode surface area, helping to upgrade the specific capacitance [30-33]. Moreover, nanostructured materials show good strain settlement that advances good cycle life and larger electrode-electrolyte surface area driving to fast charge-discharge rates [34-46]. Among them, perovskite based nanostructures have received widespread consideration recently. Perovskite is a mineral of calcium titanium oxide, which composed of calcium titanate, with formula $CaTiO_3$ [47]. Perovskites showed variety of physical and chemical characteristics such as ionic conductivity [48], electrically dynamic structure, electronic conductivity [49], superparamagnetic [50], photocatalytic [51], thermoelectric, and dielectric properties [52]. Their structural arrangements can include the ions of different size and charge, which tend to be extremely adaptable in composition [53]. Consequently,

energy bands of perovskites are highly abnormal and their composition is special in terms of characteristics [54]. Since of the truth that most of the elements within the Periodic Table can be well built within the perovskite structure [55]. They are interesting nanomaterials in catalysis [56-60], fuel cells [61-66], electrochemical sensing [67-71], energy power gadget and many applications [72-74]. The catalysis of these perovskite-type oxide is greater than that of numerous transition metals compounds and indeed a few valuable metal oxides [75]. Nano-perovskites are well known for detecting amino acids, acetone, glucose, H_2O_2 , alcohols, gases and neurotransmitters [76-78].

Perovskite based nanostructured materials are supposed to be promising, fascinating electrode materials for designing supercapacitors with high energy storage performance [79]. In this review article, the recent progress and advances in designing perovskite based nanostructured supercapacitor electrode materials is discussed, which may provide as a guidelines for the next generation of supercapacitor electrode design.

Perovskite materials: Geologist, Gustav Rose discovered the calcium titanium oxide mineral within the Urals in 1839 and it had been called perovskite in honor of Count Lev Alexevich von Perovski, a prominent Russian mineralogist. Goldschmidt first depicted the eminent crystal structure of perovskite in 1926 [80-83]. The general chemical formula for perovskite compounds is ABX_3 , where 'A' and 'B' are two cations, regularly of exceptionally different sizes and X is the anion normally oxides or halogens that bind to both cations. The 'A' atoms are usually bigger than the 'B' particles where the B particle is encompassed by an octahedron of X particles. There are different forms of perovskites in the earth's crust and the most inexhaustible ones are $MgSiO_3$ and $FeSiO_3$ [76,80,847].

Crystallography: The perovskite structures can be obtained from numerous oxides with the chemical formula ABO_3 . In chemical formula ABO_3 , A ion is an alkali earth metals or lanthanides with larger radius, B is a transition metal ion with small radius and O is the oxygen ion with the ratio of 1:1:3 [85]. Ion (A) is found at the body center, while ion (B) is found at the cube corner position and oxygen atoms are found at face-centered positions in the ABO_3 cubic unit cell of perovskite [50]. The six-fold coordination of B cation (octahedron) and the 12-fold coordination of the A cation come from the stabilization of the perovskite structure [81,84,85].

To test the reasonableness of the combination of cations for the perovskite structure, the tolerance factor can be measured. Many researchers [86-90] exclusively indicated that it is possible to determine the perovskite structure on the basis of tolerance factor values. For $1.00 < t < 1.13$, $0.9 < t < 1.0$, and $0.75 < t < 0.9$, the perovskite structure is hexagonal, cubic and ortho-rhombic, respectively. A few distortions may be found in the perfect cubic frame of perovskite brought about in ortho-rhombic, rhombohedral, hexagonal and tetragonal shapes (Fig. 1) [91]. This distortion results from the smaller particle A, which allows the BX_6 octahedra to be tilted in arrange to maximize A-X bonding. The perovskite formula must have impartial balanced charge, such that the product of the addition of the charges of A and B particles should be proportionate to the total oxygen particle charge [92-96]. A sufficient charge dispersion

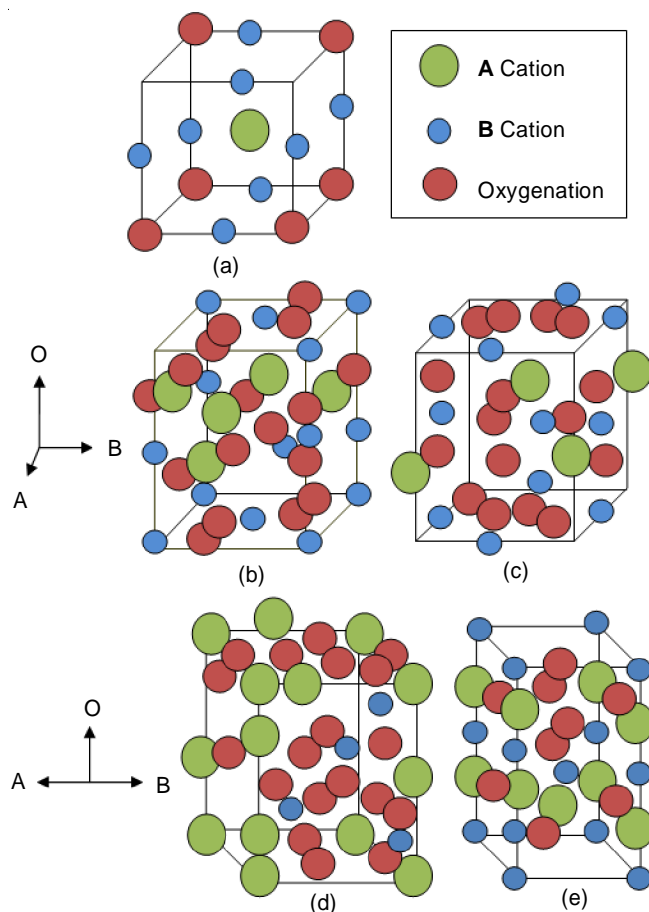


Fig. 1. Different distorted perovskite unit cells; (a) perfect lattice, (b) tetragonal, (c) orthorhombic, (d) hexagonal, (e) rhombohedral [91]

ought to be achieved in the forms of $A^{2+}B^{4+}X_3^{2-}$ or 2:4 perovskites; $A^{3+}B^{3+}X_3^{2-}$ or 3:3 perovskites; and $A^{+}B^{5+}X_3^{2-}$ or 1:5 perovskites [97-100]. Using pulsed laser deposition, molecular beam epitaxy and other methods, perovskite can be used as an epitaxial film on top of other perovskites [101-105]. It can be organized in layers, and the ABO_3 structure can be isolated by thin interlayer materials [86,97,101].

Properties: Perovskite materials display numerous properties because of its unique chemical properties such as their non-stoichiometry of their anions and/or cations, the valence mixture electronic structure, the distortion of the cation arrangement, and the mixed valence [106-111]. Dielectric properties are very properties of perovskites [112-115]. Usually, layers of these substances are introduced into capacitors to advance their execution [101]. Since it exhibits incredible resistance to current channels under the action of applied current and voltage and is strongly separated from conductive materials in basic electrical properties [116-120]. The disclosure of ferroelectricity in perovskite-based materials and other barium titanate ($BaTiO_3$) [121] has been made available for a variety of purposes, such as ultrasonic imaging systems, infrared cameras, fire sensors, vibration sensors, *etc.* [122-124]. Due to the presence of superconductivity, the oxide perovskite structure form gives a great auxiliary device. High electronic conductivity is shown by perovskites, so they are used as cathodes in solid oxide fuel cells that display prevalent hole

conductivity [125]. Fabulous catalytic activity and high chemical stability have appeared; it subsequently incorporates into the catalysis of altered reactions [126]. In addition, it can be characterized as an oxidation or oxygen-activated catalyst and as a model of dynamic sites [127,128].

Perovskite based electrode materials for designing supercapacitors: Perovskite-based nanostructures have been widely considered because of their great physical and chemical properties, including supermagnetic [50], electronic conductivity [129], ionic conductivity [130], electrically active structure [131], photocatalytic [132], thermoelectric and dielectric properties, *etc.* [133]. Hence, perovskite based nanostructured materials are supposed to be promising, fascinating electrode materials for designing supercapacitors with high energy storage performance. Herein, we reviewed perovskite based electrode materials for supercapacitors in different ways. One is based on type of perovskite and the other is based on method of perovskite synthesis.

Types of perovskite based electrode materials: Perovskite can be broadly classified into two, oxide perovskite and halide perovskite. Perovskite oxides with formula ABO_3 or A_2BO_4 are a significant class of useful materials that demonstrate the degree of stoichiometry and crystal structures [134,135]. Normal structures (ABO_3) comprise of large 12-coordinated A-site cations and small 6-coordinated B-site cations [84,85]. The common chemical formula for halide perovskite compounds is ABX_3 , where 'A' and 'B' are two cations, frequently of exceptionally different sizes, and X is halogen bonding to both cations [136,137]. Halide perovskites is identified as one of the most fascinating electrode materials for supercapacitors.

Oxide perovskite: Perovskite oxide has attracted widespread consideration as capacitor terminal materials due to its special physical and electronic properties. A novel $La_{0.7}Sr_{0.3}CoO_{3-\delta}$ (LSC)@ MnO_2 core-shell nanorod was synthesized by He *et al.* [138]. Grid-like MnO_2 nanosheets are developed on LSC to create a one of a kind core/shell nanostructure, may successfully progress the electrochemical execution of MnO_2 . These MnO_2 nanosheets shell essentially increment the effective area over which the reaction will take place and decrease the transmission distance of ions/electrons, which is helpful in moving particles and electrons, improving the kinetics of electrochemical reactions. This core/shell nanorods illustrated great electrochemical execution with high capacitance, 570 F

g^{-1} at 1 A g^{-1} and great cycle stability, capacitance maintenance remains at 97.2% after 5000 cycles. Mo *et al.* [139] developed Ca-doped perovskite lanthanum manganites ($La_{1-x}Ca_xMnO_3$, LCMs), appeared great energy storage properties. Samples doped with 50% calcium appeared prevalent specific capacitances of 170 F g^{-1} , at current thickness of 1 A g^{-1} in 1M KOH aqueous solution. The oxygen vacancies in the perovskite are considered to be the charge storage region of the pseudo capacitance. Charge storage of oxygen intercalation progressed by doping with components of low valence in perovskite manganites. Energy densities of perovskite supercapacitors will subsequently be maximized by expanding the vacancies of oxygen.

Bavio *et al.* [140] investigated the potential energy ability in supercapacitors containing oxide $La_2B(II)MnO_6$ (with B = Cu, Co, Ni) as the electrode material. The double perovskites of the $La_2B(II)MnO_6$ system can be utilized in supercapacitors as electrode material giving specific capacitance values of 700 F g^{-1} when B is Cu in alkaline solution. The higher capacitance values were gained for La_2CuMnO_6 and its specific capacitance of 781.25 F g^{-1} at a current density of 3.12 A g^{-1} and power density 72.6 kW kg^{-1} . Ho & Wang [141] developed a novel hydrazine reduction method to convert perovskite oxides into active materials with the required electrical conductivity and electrochemical behavior in order to advance the electrical conductivity and general action of active materials in pseudocapacitors. They reported one step hydrazine reduction process, which can partially convert part of the $LaNiO_3$ (LNO) into nickel oxide/hydroxide on the surface while maintaining the porous interconnected electrical conductivity structure (Fig. 2). Various hydrazine reduction durations are added to $LaNiO_3$ (LNO), leading to a significant increment in specific capacitance of 280 F g^{-1} at 1 A g^{-1} . The required electrical conductivity of LNO has been retained, as appeared by the overall resistance of less than 0.3 Ω within the aqueous electrolyte. The hydrazined LNO illustrated the specified stability as electrode, where the permeable structure offers good electrolyte openness, which supports the improvement of general electrochemical behaviours. A simple hydrothermal synthetic method has been developed for the preparation of perovskite lanthanum aluminate ($LaAlO_3$) and reduced graphene oxide composite (rGO). The rGO/ $LaAlO_3$ composite material has exhibited improved specific capacitance (721 F g^{-1} at a filter rate of 2 mV s^{-1}). The composite appeared energy density of 57 Wh kg^{-1} with power density of

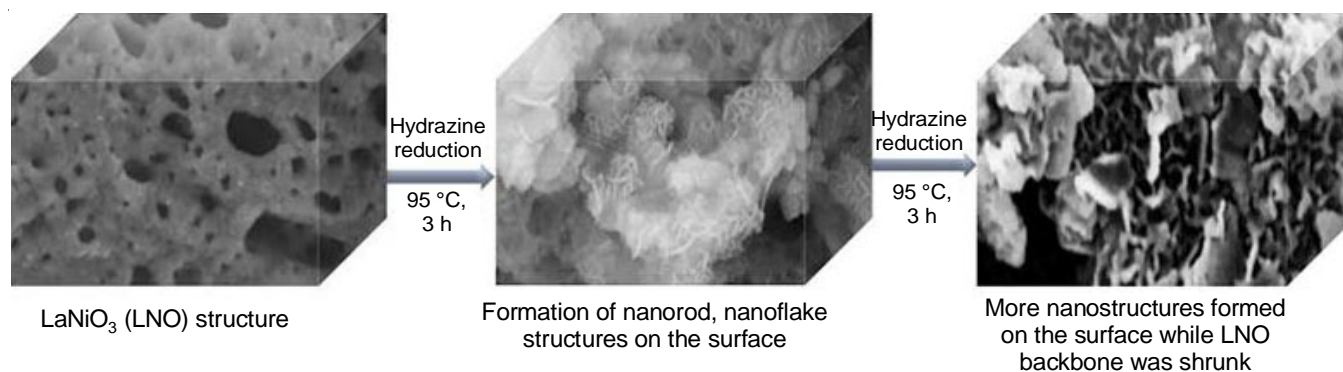


Fig. 2. Transformation of the LNO scaffold after the hydrazine reduction at 95 °C for different time span [141]

569 W kg⁻¹ [142]. Perovskite oxides are profoundly excellent electrodes for oxygen-ion-intercalation-type supercapacitors due to their high oxygen vacancy concentration and tap density. Xu *et al.* [143] synthesized B-site cation-ordered Ba₂Bi_{0.1}Sc_{0.2}Co_{1.7}O_{6.8} as an electrode material with high oxygen vacancy concentration and oxygen dissemination rate. It appeared specific capacitance of 780 F g⁻¹, energy density of 70 Wh kg⁻¹ at the power density of 787 W kg⁻¹ with an aqueous alkaline arrangement, 6 M KOH electrolyte.

Halide perovskite: The purpose of establishing self chargeable supercapacitors in electric vehicles is to reduce the emission of undesirable gases, which can be achieved by adding perovskite solar cells to self-charge the supercapacitors. CsPb Br_{2.9}I_{0.1} perovskite-sensitized solar cell is coordinated for the first time with an asymmetrical supercapacitor for a photo supercapacitor applications. The use of an inorganic cesium-based perovskite material and the useful impact of consolidating a miniature sum of iodide into the bromide system progressed the film's compactness and essentially progressed the steadiness of a solar cell. The asymmetrical supercapacitor shows a great specific capacitance of 150 mF cm⁻², which appears its potential for the photo-supercapacitor applications [144]. Slonopas *et al.* [145] illustrated the effective applications of a CH₃NH₃PbI₃ perovskite material as a dielectric capacitor with execution proportionate to asymmetric supercapacitors. A high specific capacitance of 523 mF cm⁻² was reported at 350 K and stable capacitance of 432 mF cm⁻² was kept up at room temperature. So, perovskite materials are reasonable for using as energy storage gadgets in applications requesting great extending thermal and electrical characteristics.

Organometallic halide perovskites display curiously ionic responses apart from its exceptional electronic property. These properties are utilized in manufacturing the electrochemical capacitors. Oloore *et al.* [146] developed cadmium sulfide quantum dots, organohalides perovskite-based bilayer electrodes and a perfect CdS electrodes for supercapacitors. The specific capacitance of the electrodes is improved by coating layers of methyl ammonium lead iodide and methyl ammonium bismuth iodide on the CdS quantum dots. Perovskite materials contribute additional charges and progress ionic conductivity with its crystals which leads to the progressed performance. Moreover, organometallic halide perovskites can give more dynamic sites for the electrochemical responses, shortening the pathways for transport of the charges or particles. Electrodes showed highest areal capacitance of 141 μF cm⁻² and highest energy density of 23.8 nWh cm⁻². Maji *et al.* [147] created a symmetric supercapacitor with CsPbI₃ as electrode material to illustrate

the charge storing capability. CsPbI₃ was synthesized by experimentally hazard-free chemical synthesis way, which is steady in orthorhombic stage. The device appeared great electrochemical properties with specific capacitance 7.23 mF cm⁻² at a scan rate 2mV s⁻¹ and 65.5% cyclic stabilities after 1000 cycles. In other work, supercapacitors were successfully constructed by utilizing composite materials of metal halide hybrid perovskites (MBI and MPI) and nickel oxide nanoparticles. In order to make a complete supercapacitor device, a thin layer of electrolyte is coated on the electrodes, and two identical electrodes are fixed together by two adhesive clips (Fig. 3). It was found that in expansion to the improved capacitive contribution, the sum of charge stored from proton intercalation forms with addition of perovskite materials too increased. Charge stored at the surface of MBI@NiO and MPI@NiO from the pseudocapacitance routes is a critical figure in accomplishing high values for their energy densities. The specific capacitances of 407 F g⁻¹ and 368 F g⁻¹, with comparing energy densities of 56.5 Wh kg⁻¹ and 51.1 Wh kg⁻¹ have been observed for MBI@NiO and MPI@NiO composite electrodes, separately, at 10 mV s⁻¹ [148]. Andricevic *et al.* [149] created a shining, light-emitting electrochemical cell with CH₃NH₃PbBr₃ single crystals directly developed on vertically adjusted carbon nanotube as contact terminals. The diminished interface energy barrier and the strong charge infusion due to the carbon nanotube tip upgraded electric field. The green light emitted at room temperature is as high as 1800 cd m⁻². A summary of perovskite based electrode materials (based on oxides and halides) in supercapacitors are given in Table-1.

Effect of synthetic methodology in choosing electrode materials: Perovskite is usually synthesized by solid-phase ceramic reaction. The solid-phase reaction has many disadvantages, such as product homogeneity, defects related to luminescence, and chemical pollution introduced during repeated tapping and heating operations [150,151]. In order to progress synthesis strategies and avoid these drawbacks, a few modern strategies have been suggested, such as hydrothermal synthesis, precipitation method, sol-gel method, wet chemical method, *etc.*

Hydrothermal synthesis: The hydrothermal synthesis is carried out the reaction in the aqueous solution and suspend the precursors at high temperature, pressure, without calcinations to obtain crystalline powder [152,153]. NiMnO₃ perovskite oxide with a high particular surface area and electrochemical properties was produced by means of hydrothermal synthesis at low temperature. The shape and composition were directed by controlling temperature and time of the hydrothermal synth-

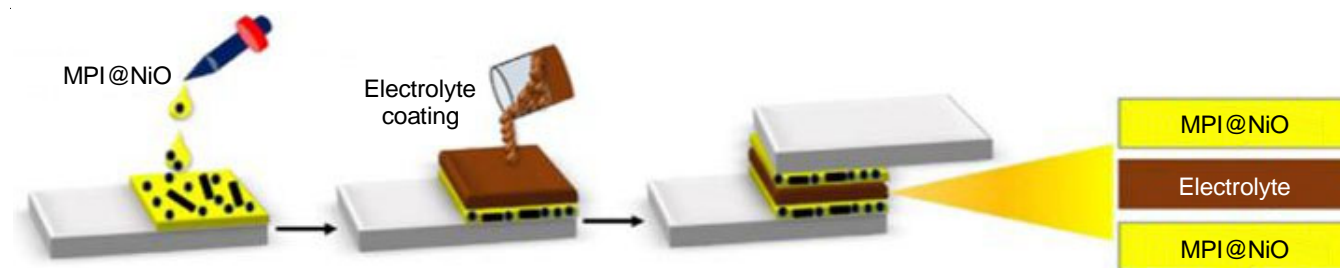


Fig. 3. Schematic representation of fabrication of supercapacitor based on MBI@NiO&MPI@NiO nanocomposites [148]

TABLE-1
PEROVSKITE BASED ELECTRODE MATERIALS IN SUPERCAPACITORS (BASED ON TYPES)

Electrode materials	Electrolyte	Specific capacitance	Power density	Energy density	Retention capability	Ref.
(i) Oxide perovskite based materials						
$\text{La}_{0.7}\text{Sr}_{0.3}\text{CoO}_{3.6}\text{@MnO}_2$	6 M KOH	570 F g ⁻¹	7489.3 W kg ⁻¹	37.6 Wh Kg ⁻¹	97.2% after 5000 cycles	[138]
$\text{La}_{1-x}\text{Ca}_x\text{MnO}_3$	1 M KOH	170 F g ⁻¹	–	–	7.7 % after 2000 cycles	[139]
$\text{La}_2\text{B(II)MnO}_6$	0.5 M KOH	781.25 F g ⁻¹	72.6 kW kg ⁻¹	113.4 Wh kg ⁻¹	–	[140]
LaNiO_3	1 M KOH	280 F g ⁻¹	–	–	–	[141]
rGO/LaAlO ₃	1 M Na ₂ SO ₄	721 F g ⁻¹	569 W kg ⁻¹	57 Wh kg ⁻¹	85% after 3000cycles	[142]
$\text{Ba}_2\text{Bi}_{0.1}\text{Sc}_{0.2}\text{Co}_{1.7}\text{O}_{6.6}$	6 M KOH	1050F g ⁻¹	787 W kg ⁻¹	70 Wh kg ⁻¹	92% after 2000 cycles	[143]
(ii) Halide perovskite based materials						
$\text{CsPbBr}_3/\text{I}_{0.1}$	–	150 mF cm ⁻²	–	–	–	[144]
$\text{CH}_3\text{NH}_3\text{PbI}_3$	–	523 mF cm ⁻²	–	57 Wh Kg ⁻¹	–	[145]
CdS-MAPI_3	–	141 μF cm ⁻²	12.7 mW cm ⁻²	23.8 nWh cm ⁻²	87 % after 4000 cycles	[146]
CsPbI_3	–	7.23mF cm ⁻²	–	–	65.5% after 1000 cycles	[147]
$\text{MBI@NiO}\&\text{MPI@NiO}$	–	407 F g ⁻¹ & 368 F g ⁻¹	–	56.5 Wh Kg ⁻¹ & 51.1 Wh Kg ⁻¹	90% after 3000 CV cycles.	[148]
$\text{CH}_3\text{NH}_3\text{PbBr}_3$	–	507 F g ⁻¹	764 W kg ⁻¹	–	–	[149]

esis reaction. To change the specific surface range and morphology, the synthesis of perovskite oxide was regulated by the reaction time. It appeared a high specific capacitance of 99.03 F g⁻¹ and fabulous cycle stability with a coulombic efficiency of 77% indeed after 7000 cycles. Thus, synthesized perovskite can be utilized as an dynamic electrode for supercapacitors [154]. Hydrothermally synthesized LaFeO₃ perovskite (LF) is co-doped with Mn and Nd to form La_{0.8}Nd_{0.2}Fe_{0.8}Mn_{0.2}O₃ (LNFM), which have higher specific capacitance of 158 F g⁻¹ at 50 mV/s compared to non-doped and single doped LF samples. The coexistence of ferrite powders and graphene oxide (NGO) doped with LNFM/nitrogen improves nanocomposite specific capacitance by more than 7 times. It has been found that the emergence of NGO greatly increases the specific capacitance of nanocomposites to 1060 F g⁻¹ at 50 mV s⁻¹. After 10000 non-stop cycles, composite showed exceptional capacity retention as 92.4% [155].

Singh *et al.* [156] effectively prepared La₂ZnMnO₆ nanofakes through simple hydrothermal method. Electron diffraction pattern of the compound represents the arrangement of diffraction rings relative to the orthogonal structure. At normal hole distance 12 nm, the measured specific surface area is 46 m² g⁻¹ and specific capacitance is 718.6 F g⁻¹ at a scan rate of 1 mV s⁻¹. The nanofake electrode exhibited retention of ~86% specific capacitance after 1000 cycles at a steady current density of 2.5 A g⁻¹. Nagamuthu *et al.* [157] have developed CeO₂ mixed LaMnO₃ nanocomposites, which showed mesopore size and high surface region within the N₂ adsorption/desorption measurements. Three terminal measurements indicate that the CeO₂ mixed LaMnO₃ nanocomposites is an appropriate negative electrode fabric for supercapacitor. The specific capacitance and energy density of asymmetric supercapacitor are found to be 262 F g⁻¹ at a constant current of 1 A g⁻¹ and 17.2 Wh kg⁻¹ at a power density of 1015 w kg⁻¹, respectively. A new type of perovskite oxide Ba_xMn_{1-x}O₃ electrode for supercapacitors was fabricated *via* the hydrothermal synthesis with changing concentration of Ba. The surface region of the nanorods has been extended to increase the concentration of dopant, which constantly

increases the electrochemical characteristics. It exhibited high specific capacitance of 433 F g⁻¹ and high retention capacitance as 104% after 1000 cycles. In addition, prepared BaMnO₃ has good conductivity with charge exchange resistance and successful series resistance of 2.9 and 4 Ω [158].

Precipitation method: The precipitation of metal salts may be a strategy, usually used to synthesize perovskites [159]. Precipitation arises after the chemical reagent is used, which diminish the solubility limit [160]. Harikrishnan & Bose [161] synthesized LaNiO₃ through co-precipitation strategy and the samples were strengthened at distinctive temperatures. The X-ray diffraction results show the crystallinity and rhombohedral stage and the morphological characteristics of the sample exhibits non-homogenous nature and twisted spherical structure. The high capacitance values of the electrode are measured to be 206.37 F g⁻¹ at scan rates of 2 mV s⁻¹ and 212.86 F g⁻¹ at current density of 2 A g⁻¹, respectively in 3M KOH electrolyte, which resulted in lower aggregation, higher particle diffusion and greater electrical conductivity. This opens an entry way for manufacturing electrodes for high-performance energy storage gadgets. In other work, a basic chemical precipitation strategy was utilized to synthesize pure-phase KCoF₃ having a size of 1-5 μm, which is used in supercapacitors. Due to the oxidation-reduction reaction of Co particles, supercapacitors based on KCoF₃ exhibits great energy storage capacity. The electrode showed long cycle life with 96% retention after 1000 cycles at a current density of 5.0 A g⁻¹ and specific capacitance of 286 F g⁻¹ at 0.5 A g⁻¹ in 6.0 M KOH electrolyte [162]. Cheng *et al.* [163] built a clustered countercurrent-flow micro-channel reactor for the synthesis of KMnF₃ perovskite fluoride by a co-precipitation method. The morphologies and electrochemical characteristics of the synthesized KMnF₃ particles have been changed accordingly with the micromixing efficiencies of clustered micro-channel countercurrent-flow reactor, which can be balanced by the configuration and working conditions of the reactor. Here, KMnF₃ acts as positive electrode, activated carbon as negative electrode and also 2 M KOH and non-woven slice are used as electrolyte and separator, respectively (Fig. 4).

An asymmetric supercapacitor gathered with the KMnF_3 and activated carbon displayed an energy density of 13.1 W h kg^{-1} at a power density of 386.3 W kg^{-1} , specific capacitance of $\sim 442 \text{ F g}^{-1}$ at a current density of 1 A g^{-1} , with prominent capacitance retention of $\sim 81.2\%$ after 5000 cycles.

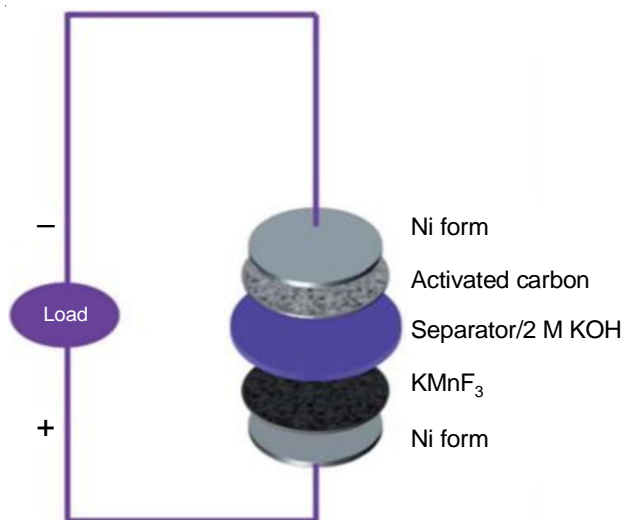


Fig. 4. Schematic of the assembled asymmetric supercapacitor based on KMnF_3 perovskite [163]

A high execution supercapacitor was manufactured using LaCoO_3 electrode synthesized by co-precipitation strategy. The XRD result confirmed the crystalline nature of the rhombohedral LaCoO_3 phase and morphological studies exhibit distorted polyhedron shape. The specific capacitance of LaCoO_3 electrode showed 532.55 F g^{-1} at scan rate 10 mV s^{-1} and 299.64 F g^{-1} at current density 10 A g^{-1} reveals a greater particle diffusion and exceptional electronic conductivity [164].

Lannelongue *et al.* [165] reported two asymmetric aqueous electrochemical capacitors, $\text{C}/\text{Ba}_{0.5}\text{Sr}_{0.5}\text{-Co}_{0.8}\text{Fe}_{0.2}\text{O}_{3-8}$ (BSCF) and $\text{FeWO}_4/\text{BSCF}$ with activated carbon, synthesized by a precipitation strategy. These two devices were worked between and 1.6 V and between and 1.4 V , individually. At low current density, the volume energy density of the device is as high as 2.7 Wh L^{-1} . Both gadgets displayed long cycle life with capacitance retention of 88% over 10,000 cycles for the C/BSCF gadget and 83% over 45,000 cycles for the $\text{FeWO}_4/\text{BSCF}$ device. In other work, the CeNiO_3 material was prepared through co-precipitation strategy as a pseudocapacitor electrode. The electrode shows greatest specific capacitance of 510 F g^{-1} at a current density of 1 A g^{-1} . The electrode keeps up 79% rate capability indeed at current density of 25 F g^{-1} additionally features a cyclic stability of 97% maintenance after 5000 cycles at current thickness of 15 A g^{-1} . The CeNiO_3 appeared to be an excellent electrode material for supercapacitor applications [166].

Sol-gel method: The sol-gel strategies are well set in the preparation of complex oxides because they can obtain pure phase products and precisely control their stoichiometry [167]. This quality makes them a device of choice for the synthesis of perovskite-type oxides. Elsiddig *et al.* [168] designed and synthesized non-stoichiometric $\text{LaMn}_{1-x}\text{O}_3$ perovskite materials

by a simple sol-gel strategy and applied as supercapacitor electrodes. This mesoporous morphology encourages quick particle diffusion and electron exchange at the electrode/electrolyte interface. $\text{LaMn}_{1.1}\text{O}_3$ sample exhibited much higher particular capacity $202.1 \text{ mAh g}^{-1}/727.6 \text{ C g}^{-1}$ at 1 A g^{-1} . Sharma *et al.* [169] also developed a Mo-doped strontium cobaltite ($\text{SrCo}_{0.9}\text{Mo}_{0.1}\text{O}_{3-8}$, SCM) and prepared as an oxygen anion-intercalated type charge storage material through sol-gel strategy. Here O^{2-} diffusion as the rate constraining factor for charge capacity. Electrode exhibited great energy and power density, 74.8 Wh kg^{-1} , 6600 W kg^{-1} as well exceptional cycling life, holding 97.6% initial specific capacitance after 10,000 cycles at 10 A g^{-1} . In other work, high-crystalline SrMnO_3 perovskite oxide nanofibers have been successfully constructed by George *et al.* [170]. It was developed by sol-gel electrospinning, using poly(vinyl pyrrolidone) as a sacrificial polymeric binder. Doping 20 mol% Ba to SrMnO_3 lattice completely increases the specific capacitance from 321.7 F g^{-1} to up to 446.8 F g^{-1} . It can be considered that the increase in specific capacitance caused by doping is an increase in oxygen vacancies caused by lattice distortion. The nanofibers showed energy density of 37.3 Wh kg^{-1} at a power density of 400 W kg^{-1} . The nanofibers held 87% its initial capacitance after 5000 successive cycles and recognize them as a excellent candidate for supercapacitors.

Tomar *et al.* [171] demonstrated the extraordinary charge capacity characteristics of strontium titanate with cubic structure utilizing sol-gel synthesis and investigated in both aqueous and solid state supercapacitor as charge storage material. Cubic structure of perovskite is valuable for supercapacitors because of its three-dimensional diffusion channels for oxygen anion diffusion. Strontium titanate electrode showed high capacitance of 592 F g^{-1} due to its longer particular surface range and exceptional mass exchange rate of electrolytic particles. The symmetric cell in aqueous media showed greatest energy and power density 27.8 Wh kg^{-1} and 1921 W kg^{-1} with great cycle stability, 99% capacitance maintenance after 5000 GCD cycles. An extraordinary working electrode developed utilizing mesoporous cobalt titanate (CTO) microrods through the sol-gel route. The mesoporous CTO microrods with expanded textural boundaries played a crucial role within the diffusion of particles and contributed specific capacitance of 608.4 F g^{-1} , specific power of 4835.7 W kg^{-1} and a specific energy of 9.77 Wh kg^{-1} in an aqueous 2 M KOH electrolyte. The mesoporous CTO appears its potential as an electrode for a long-cycle supercapacitor and gives openings for extra improvement after creating the core-shell hetero-architecture with other metal oxide materials such as MnO_2 and TiO_2 [172]. Kitchamsetti *et al.* [173] synthesized mesoporous nickel titanite (NTO) rods including progressively interlocked nanoparticles as an amazing electrode for the applications of supercapacitor. It appeared specific capacitance of 542.26 F g^{-1} , the energy density of 8.06 Wh kg^{-1} and a power density of 4320 W kg^{-1} , which is essentially superior than Ni, Mn, Fe, Cr and Ti-based perovskites. The diffusion-controlled mechanism is faster and upgraded get to the OH^- particles profound interior the rod body, showed long life cycle, high stability up to 2100 cycles.

Wet chemical method: Wet chemical method is an effective precise synthetic technique for synthesizing the redox state of double-perovskite compound [76]. These methods including the sol-gel synthesis, co-precipitation of metal particles utilizing distinctive precipitating agents and warm treatment [174]. Wet chemical strategies were categorized built on the strategies utilized for solvent removal [175]. New oxygen-deficient double perovskites, $\text{Ba}_2\text{FeCoO}_{6-\delta}$, was synthesized using simple wet chemical synthesis. The specific capacitance of $\text{Ba}_2\text{FeCoO}_{6-\delta}$ is 820.0 F g^{-1} at a current density of 3 A g^{-1} . The electrode gives values of energy and power densities as 23.06 Wh kg^{-1} and 677.92 W kg^{-1} , exhibiting potential of $\text{Ba}_2\text{FeCoO}_{6-\delta}$ electrode for supercapacitive applications [176]. Mansoori *et al.* [177] reported a simple chemical synthesis of novel double perovskite Y_2CuMnO_6 nanocrystallites by a wet chemical sol gel method. X-ray photoelectron spectra showed the nearness of Y^{3+} , Cu^{2+} and Mn^{4+} species at the surface of the Y_2CuMnO_6 . The specific capacitance $\sim 15.6 \text{ F g}^{-1}$, energy density $\sim 0.43 \text{ Wh kg}^{-1}$ and power density $\sim 56.2 \text{ W kg}^{-1}$ have been observed at the current thickness of 0.2 A g^{-1} . The Y_2CuMnO_6 nanocrystallites anode appeared specific capacitance maintenance of $\sim 75\%$ for 1000 cycles. The novel double perovskite Y_2CoNiO_6 was successfully synthesized by ethylene glycol and citric acid stabilized effortless wet sol-gel chemical method. In the sample with second-order phase transition, an over-whelming paramagnetic behaviour was obtained. The effective charge capacity was due to redox response of $\text{Co}^{2+}/\text{Co}^{3+}$ and $\text{Co}^{3+}/\text{Co}^{4+}$ as promoted by X-ray photoelectron spectroscopy. Power and energy densities

of Y_2CoNiO_6 were 19.97 Wh kg^{-1} and 1324 W kg^{-1} , respectively [178].

Kumar *et al.* [179] were effectively developed double perovskite $\text{Gd}_2\text{NiMnO}_6$ through simple wet chemical process. The X-ray photoelectron spectroscopy studies displayed the nearness of Gd^{3+} , $\text{Ni}^{2+}/\text{Ni}^{3+}$, $\text{Mn}^{2+}/\text{Mn}^{3+}/\text{Mn}^{4+}$ particles on the surface of $\text{Gd}_2\text{NiMnO}_6$. It has appeared specific capacitance of 400.46 F g^{-1} at the current density of 1 A g^{-1} . Energy density of 20.23 Wh kg^{-1} and power density of 421.75 W kg^{-1} have been obtained, which appear potential of electrode fabric for the energy storage gadgets. Singh *et al.* [180] synthesized new synthesis route accompanying improvement of new anode fabric with potential of application in next generation energy storage gadgets. Double perovskite $\text{La}_2\text{FeCoO}_6$ nanocrystallites prepared through wet chemical sol-gel method. The nanocrystallites electrode displayed specific capacitance of 831.1 F g^{-1} at current thickness of 1 A g^{-1} . In addition, $\text{La}_2\text{FeCoO}_6$ nanocrystallites have appeared energy density $\sim 23.3 \text{ Wh kg}^{-1}$ and power density $\sim 224.9 \text{ W kg}^{-1}$ at current thickness of 1 A g^{-1} . In other work, a hybrid $\text{WO}_3\text{-ZnS}$ nanocomposite was prepared by microwave-assisted wet chemistry strategy, and the composite was used to improve the capacitance execution of WO_3 via compositing. SEM and HRTEM studies showed that as-prepared nanocomposites comprised of irregular particles of moderate size. The hybrid state of the orthorhombic and cubic structure of WO_3 and cubic structure of ZnS was distinguished, and its molecular size was getting diminished by stacking ZnS into WO_3 . Charge-discharge analysis appeared

TABLE-2
PEROVSKITE ELECTRODE MATERIALS IN SUPERCAPACITORS (BASED ON SYNTHESIS)

Electrode materials	Electrolyte	Specific capacitance	Power density	Energy density	Retention capability	Ref.
(i) Hydrothermal synthesis						
NiMnO_3	6 M KOH	99.03 F g^{-1}	–	–	77% after 7000 cycles	[154]
$\text{La}_{0.8}\text{Nd}_{0.2}\text{Fe}_{0.8}\text{Mn}_{0.2}\text{O}_3/\text{NGO}$	3 M KOH	1060 F g^{-1}	–	–	92.4% after 10000 cycle	[155]
$\text{La}_2\text{ZnMnO}_6$	2 M KOH	718.6 F g^{-1}	–	–	86%after 10000 cycle	[156]
$\text{LaMnO}_3/\text{CeO}_2$	1 M Na_2SO_4	262 F g^{-1}	1015 w kg^{-1}	17.2 Wh kg^{-1}	92% after 20000 cycle	[157]
$\text{Ba}_x\text{Mn}_{1-x}\text{O}_3$	1 M KOH	433 F g^{-1}	–	–	104% after 1000 cycles	[158]
(ii) Precipitation method						
LaNiO_3	3 M KOH	212.86 F g^{-1}	–	–	–	[161]
KCoF_3	6 M KOH	286 F g^{-1}	–	–	96%after 10000 cycle	[162]
KMnF_3	2 M KOH	442 F g^{-1}	386.3 W kg^{-1}	13.1 Wh kg^{-1}	81.2% after 5000 cycles	[163]
LaCoO_3	3 M KOH	532.55 F g^{-1}	–	–	–	[164]
$\text{C}/\text{Ba}_{0.5}\text{Sr}_{0.5}\text{Co}_{0.8}\text{Fe}_{0.2}\text{O}_{3-d}$	5 M LiNO_3	46 C g^{-1}	–	2.7 Wh L^{-1}	83% after 45,000 cycles	[165]
CeNiO_3	3 M KOH	510 F g^{-1}	–	–	97% after 5000 cycles	[166]
(iii) Sol-gel method						
$\text{LaMn}_{1-x}\text{O}_3$	1 M KOH	202 mAhg^{-1}	–	–	73% after 1000 cycles	[168]
$\text{SrCo}_{0.9}\text{Mo}_{0.1}\text{O}_{3-\delta}$	6 M KOH	1223 F g^{-1}	6600 W kg^{-1}	74.8 Wh kg^{-1}	97.6 % after 10,000 cycles	[169]
SrMnO_3	0.5 M Na_2SO_4	321.7 F g^{-1}	400 W kg^{-1}	37.3 Wh kg^{-1}	87% after 5000 cycles	[170]
SrTiO_3	3 M KOH	592 F g^{-1}	1921 W kg^{-1}	27.8 Wh kg^{-1}	71.6% after 3000 cycles	[171]
CoTiO_3	2 M KOH	608.4 F g^{-1}	4835.7 W kg^{-1}	9.77 Wh kg^{-1}	82.3% after 1950 cycles	[172]
NiTiO_3	2 M KOH	542.26 F g^{-1}	4320 W kg^{-1}	8.06 Wh Kg^{-1}	91% after 2100 cycles	[173]
(iv) Wet chemical method						
$\text{Ba}_2\text{FeCoO}_{6-\delta}$	2 M KOH	820.0 F g^{-1}	677.9 W kg^{-1}	23.06 Wh kg^{-1}	–	[176]
Y_2CuMnO_6	1 M KOH	15.6 F g^{-1}	56.2 W kg^{-1}	0.43 Wh kg^{-1}	75% after 1000 cycles	[177]
Y_2CoNiO_6	–	–	1324 W kg^{-1}	$19.97 \text{ Wh h kg}^{-1}$	98.5% after 1200 cycles	[178]
$\text{Gd}_2\text{NiMnO}_6$	4 M KOH	400.46 F g^{-1}	421.75 W kg^{-1}	20.23 Wh kg^{-1}	–	[179]
$\text{La}_2\text{FeCoO}_6$	1 M KOH	831.1 F g^{-1}	224.9 W kg^{-1}	23.3 Wh Kg^{-1}	88% after 1000 cycles	[180]
$\text{WO}_3\text{-ZnS}$	20% KOH	215 F g^{-1}	–	–	71% after 4000 cycles	[181]

the greatest capacitance of WO₃ was improved from 44 F g⁻¹ to 215 F g⁻¹ by the stacking of ZnS with WO₃ in KOH electrolyte. It appears to be an excellent material for the manufacture of supercapacitor gadgets [181]. A summary of perovskite based electrode materials (based on synthetic routes) in supercapacitors are given in Table-2.

Conclusion

Perovskite based nanostructured materials are supposed to be promising, fascinating electrode materials for designing supercapacitors with high energy storage performance. These materials have received broad consideration due to their excellent physical and chemical characteristics such as electronic conductivity, ionic conductivity, electrically active structure, supermagnetic, photocatalytic, thermoelectric, dielectric properties, *etc.* So they are interesting nanomaterials for wide applications in catalysis, fuel cells, electrochemical sensing and energy capacity gadget. The migration of ions through lattices enables perovskite nanostructures to be used as electrodes for supercapacitors. Perovskite oxide are further investigated for such applications due to their excellent energy and power density, high specific capacitance and long cycle life. Very recently the perovskite metal halides have drawn broad consideration in energy conversion and storage technology. Because it can be used as both electrolyte and electrode material in halide perovskite based supercapacitors. Thus, this article reviewed the recent progress and advances in designing perovskite based nanostructured electrode materials, which provide as a guidelines for the next generation of supercapacitor electrode design.

ACKNOWLEDGEMENTS

The authors (ASN, VJ and VJ) thank and acknowledge Karunya Institute of Technology and Sciences for providing necessary facilities to initiate “Supercapacitors Based Research Activity” in the Department of Applied Chemistry.

CONFLICT OF INTEREST

The authors declare that there is no conflict of interests regarding the publication of this article.

REFERENCES

- D. Majumdar, M. Mandal and S.K. Bhattacharya, *Emergent Mater.*, **3**, 347 (2020); <https://doi.org/10.1007/s42247-020-00090-5>
- P.J. Hall and E.J. Bain, *Energy Policy*, **36**, 4352 (2008); <https://doi.org/10.1016/j.enpol.2008.09.037>
- J.R. Miller and P. Simon, *Science*, **321**, 651 (2008); <https://doi.org/10.1126/science.1158736>
- B. Zhao, D. Chen, X. Xiong, B. Song, R. Hu, Q. Zhang, B.H. Rainwater, G.H. Waller, D. Zhen, Y. Ding, Y. Chen, C. Qu, D. Dang, C.-P. Wong and M. Liu, *Energy Storage Mater.*, **7**, 32 (2017); <https://doi.org/10.1016/j.ensm.2016.11.010>
- L.L. Zhang and X.S. Zhao, *Chem. Soc. Rev.*, **38**, 2520 (2009); <https://doi.org/10.1039/b813846j>
- E. Frackowiak and F. Beguin, *Carbon*, **39**, 937 (2001); [https://doi.org/10.1016/S0008-6223\(00\)00183-4](https://doi.org/10.1016/S0008-6223(00)00183-4)
- W. Raza, F. Ali, N. Raza, Y. Luo, K.H. Kim, J. Yang, S. Kumar, A. Mehmood and E.E. Kwon, *Nano Energy*, **52**, 441 (2018); <https://doi.org/10.1016/j.nanoen.2018.08.013>
- Q. Gou, S. Zhao, J. Wang, M. Li and J. Xue, *Nano-Micro Lett.*, **12**, 98 (2020); <https://doi.org/10.1007/s40820-020-00430-4>
- M.J. Young, A.M. Holder, S.M. George and C.B. Musgrave, *Chem. Mater.*, **27**, 1172 (2015); <https://doi.org/10.1021/cm503544e>
- B. Xu, S. Yue, Z. Sui, X. Zhang, S. Hou, G. Cao and Y. Yang, *Energy Environ. Sci.*, **4**, 2826 (2011); <https://doi.org/10.1039/c1ee01198g>
- S. Liu, L. Wei and H. Wang, *Appl. Energy*, **278**, 115436 (2020); <https://doi.org/10.1016/j.apenergy.2020.115436>
- S. Huang, X. Zhu, S. Sarkar and Y. Zhao, *APL Mater.*, **7**, 100901 (2019); <https://doi.org/10.1063/1.5116146>
- S. De, S. Acharya, S. Sahoo and G. Chandra Nayak, *Nanostructured, Functional, and Flexible Materials for Energy Conversion and Storage Systems*, Elsevier, Chap. 12, pp. 373-415 (2020); <https://doi.org/10.1016/B978-0-12-819552-9.00012-9>
- R. Kotz and M. Carlen, *Electrochim. Acta*, **45**, 2483 (2000); [https://doi.org/10.1016/S0013-4686\(00\)00354-6](https://doi.org/10.1016/S0013-4686(00)00354-6)
- P. Sharma and T.S. Bhatti, *Energy Convers. Manage.*, **51**, 2901 (2010); <https://doi.org/10.1016/j.enconman.2010.06.031>
- P.K. Panda, A. Grigoriev, Y.K. Mishra and R. Ahuja, *Nanoscale Adv.*, **2**, 70 (2020); <https://doi.org/10.1039/C9NA00307J>
- B.E. Conway, *Electrochem. Supercapacitors*, **2**, 11 (1999); https://doi.org/10.1007/978-1-4757-3058-6_2
- F. Wang, X. Wu, X. Yuan, Z. Liu, Y. Zhang, L. Fu, Y. Zhu, O. Zhou, U. Wu and W. Huang, *Chem. Soc. Rev.*, **46**, 6816 (2017); <https://doi.org/10.1039/C7CS00205J>
- M.R. Biradar, A.V. Salkar, P.P. Morajkar, S.V. Bhosale and S.V. Bhosale, *New J. Chem.*, **45**, 5154 (2021); <https://doi.org/10.1039/D0NJ05990K>
- Y. Li, M. van Zijll, S. Chiang and N. Pan, *J. Power Sources*, **196**, 6003 (2011); <https://doi.org/10.1016/j.jpowsour.2011.02.092>
- T. Esawy, M. Khairy, A. Hany and M.A. Mousa, *Appl. Phys., A Mater. Sci. Process.*, **124**, 566 (2018); <https://doi.org/10.1007/s00339-018-1967-9>
- J. Yu, N. Fu, J. Zhao, R. Liu, F. Li, Y. Du and Z. Yang, *ACS Omega*, **4**, 15904 (2019); <https://doi.org/10.1021/acsomega.9b01916>
- M.I.A. Abdel Maksoud, R.A. Fahim, A.E. Shalan, M. Abd Elkodous, S.O. Olojede, A.I. Osman, C. Farrell, A.H. Al-Muhtaseb, A.S. Awed, A.H. Ashour and D.W. Rooney, *Environ. Chem. Lett.*, **19**, 375 (2021); <https://doi.org/10.1007/s10311-020-01075-w>
- W. Chen, R.B. Rakhi, L. Hu, X. Xie, Y. Cui and H.N. Alshareef, *Nano Lett.*, **11**, 5165 (2011); <https://doi.org/10.1021/nl2023433>
- L. Caizán-Juanarena, C. Borsje, T. Sleutels, D. Yntema, C. Santoro, I. Ieropoulos, F. Soavi and A. ter Heijne, *Biotechnol. Adv.*, **39**, 107456 (2020); <https://doi.org/10.1016/j.biotechadv.2019.107456>
- J. Yan, S. Li, B. Lan, Y. Wu and P.S. Lee, *Adv. Funct. Mater.*, **30**, 1902564 (2020); <https://doi.org/10.1002/adfm.201902564>
- X. Li and B. Wei, *Nano Energy*, **2**, 159 (2013); <https://doi.org/10.1016/j.nanoen.2012.09.008>
- O.S. Okwundu, C.O. Ugwuoke and A.C. Okaro, *Metall. Mater. Trans., A Phys. Metall. Mater. Sci.*, **25**, 105 (2019); <https://doi.org/10.30544/417>
- M. Jayalakshmi and K. Balasubramanian, *Int. J. Electrochem. Sci.*, **3**, 1196 (2008).
- H. Lv, Q. Pan, Y. Song, X.-X. Liu and T. Liu, *Nano-Micro Lett.*, **12**, 118 (2020); <https://doi.org/10.1007/s40820-020-00451-z>
- M. Huang, F. Li, F. Dong, Y.X. Zhang and L.L. Zhang, *J. Mater. Chem. A Mater. Energy Sustain.*, **3**, 21380 (2015); <https://doi.org/10.1039/C5TA05523G>
- P. Ratajczak, M.E. Suss, F. Kaasik and F. Béguin, *Energy Storage Mater.*, **16**, 126 (2019); <https://doi.org/10.1016/j.ensm.2018.04.031>

33. N. Zaman, R.A. Malik, H. Alrobei, J. Kim, M. Latif, A. Hussain, A. Maqbool, R.A. Karim, M. Saleem, M. Asif Rafiq and Z. Abbas, *Crystals*, **10**, 1043 (2020); <https://doi.org/10.3390/cryst10111043>
34. R. Pitchai, V. Thavasi, S.G. Mhaisalkar and S. Ramakrishna, *J. Mater. Chem.*, **21**, 11040 (2011); <https://doi.org/10.1039/c1jm10857c>
35. R.S. Kate, S.A. Khalate and R.J. Deokate, *J. Alloys Compd.*, **734**, 89 (2018); <https://doi.org/10.1016/j.jallcom.2017.10.262>
36. A. Muzaffar, M.B. Ahamed, K. Deshmukh and J. Thirumalai, *Renew. Sustain. Energy Rev.*, **101**, 123 (2019); <https://doi.org/10.1016/j.rser.2018.10.026>
37. P. Sharma and V. Kumar, *Pramana Res. J.*, **8**, 50 (2018).
38. P. Forouzandeh, V. Kumaravel and S.C. Pillai, *Catalysts*, **10**, 969 (2020); <https://doi.org/10.3390/catal10090969>
39. K. Krishnan, P. Jayaraman, S. Balasubramanian and U. Mani, *J. Mater. Chem. A Mater. Energy Sustain.*, **6**, 23650 (2018); <https://doi.org/10.1039/C8TA09524H>
40. N.L. Wu, *Mater. Chem. Phys.*, **75**, 6 (2002); [https://doi.org/10.1016/S0254-0584\(02\)00022-6](https://doi.org/10.1016/S0254-0584(02)00022-6)
41. V. Augustyn, P. Simon and B. Dunn, *Energy Environ. Sci.*, **7**, 1597 (2014); <https://doi.org/10.1039/c3ee44164d>
42. K. Khan, A.K. Tareen, M. Aslam, A. Mahmood, Q. Khan, Y. Zhang, Z. Ouyang, Z. Guo and H. Zhang, *Progr. Solid State Chem.*, **58**, 100254 (2020); <https://doi.org/10.1016/j.progsolidstchem.2019.100254>
43. D. Majumdar, *Mater. Sci. Res. India*, **15**, 30 (2018); <https://doi.org/10.13005/msri/150104>
44. E. Frackowiak, K. Jurewicz, S. Delpeux and F. Beguin, *J. Power Sources*, **97-98**, 822 (2001); [https://doi.org/10.1016/S0378-7753\(01\)00736-4](https://doi.org/10.1016/S0378-7753(01)00736-4)
45. K. Naoi and P. Simon, *Electrochem. Soc. Interface*, **17**, 34 (2008); <https://doi.org/10.1149/2.F040811F>
46. T. Chen and L. Dai, *Mater. Today Commun.*, **16**, 272 (2013); <https://doi.org/10.1016/j.matcom.2013.07.002>
47. A. Sarfraz, A.H. Raza, M. Mirzaei, Q. Abbas and R. Raza, *Electrode Materials for Fuel Cells*, In: Reference Module in Materials Science and Materials Engineering; Elsevier: Amsterdam, The Netherlands (2020).
48. S.P. Jiang, L. Liu, K.P. Ong, P. Wu, J. Li and J. Pu, *J. Power Sources*, **176**, 82 (2008); <https://doi.org/10.1016/j.jpowsour.2007.10.053>
49. S.R. Bhandari, D.K. Yadav, B.P. Belbase, M. Zeeshan, B. Sadhukhan, D.P. Rai, R.K. Thapa, G.C. Kaphle and M.P. Ghimire, *RSC Adv.*, **10**, 16179 (2020); <https://doi.org/10.1039/C9RA10775D>
50. N. Choudhary, M.K. Verma, N.D. Sharma, S. Sharma and D. Singh, *J. Sol-Gel Sci. Technol.*, **86**, 73 (2018); <https://doi.org/10.1007/s10971-018-4593-2>
51. S.A. Kulkarni, S.G. Mhaisalkar, N. Mathews and P.P. Boix, *Small Methods*, **3**, 1800231 (2019); <https://doi.org/10.1002/smt.201800231>
52. M. Srikanth, M.S. Ozorio and J.L.F. Da Silva, *Phys. Chem. Chem. Phys.*, **22**, 18423 (2020); <https://doi.org/10.1039/D0CP03512B>
53. Q. Chen, N. De Marco, Y.M. Yang, T.-B. Song, C.-C. Chen, H. Zhao, Z. Hong, H. Zhou and Y. Yang, *Nano Today*, **10**, 355 (2015); <https://doi.org/10.1016/j.nantod.2015.04.009>
54. Q. Ou, X. Bao, Y. Zhang, H. Shao, G. Xing, X. Li, L. Shao and Q. Bao, *Nano Mater. Sci.*, **1**, 268 (2019); <https://doi.org/10.1016/j.nanoms.2019.10.004>
55. L. Theofylaktos, O.K. Kosmatos, E. Giannakaki, E. Kourti, D. Deligiannis, M. Konstantakou and T. Stergiopoulos, *Dalton Trans.*, **48**, 9516 (2019); <https://doi.org/10.1039/C9DT01485C>
56. R.J.H. Voorhoeve, D.W. Johnson Jr., J.P. Remeika and P.K. Gallagher, *Science*, **195**, 827 (1977); <https://doi.org/10.1126/science.195.4281.827>
57. A. Grimaud, K.J. May, C.E. Carlton, Y.L. Lee, M. Risch, W.T. Hong, J. Zhou and Y. Shao-Horn, *Nat. Commun.*, **4**, 2439 (2013); <https://doi.org/10.1038/ncomms3439>
58. H. Zhu, P. Zhang and S. Dai, *ACS Catal.*, **5**, 6370 (2015); <https://doi.org/10.1021/acscatal.5b01667>
59. J. Hwang, R.R. Rao, L. Giordano, Y. Katayama, Y. Yu and Y. Shao-Horn, *Science*, **358**, 751 (2017); <https://doi.org/10.1126/science.aam7092>
60. X. Xu, Y. Zhong and Z. Shao, *Trends Chem.*, **1**, 410 (2019); <https://doi.org/10.1016/j.trechm.2019.05.006>
61. J.T.S. Irvine, *Fuel Cells and Hydrogen Energy*, 167 (2009); https://doi.org/10.1007/978-0-387-77708-5_8
62. X.P. Wang, D.F. Zhou, G.C. Yang, S.C. Sun, Z.H. Li, H. Fu and J. Meng, *Int. J. Hydrogen Energy*, **39**, 1005 (2014); <https://doi.org/10.1016/j.ijhydene.2013.10.096>
63. M. Lo Faro and A.S. Aricò, *Int. J. Hydrogen Energy*, **38**, 14773 (2013); <https://doi.org/10.1016/j.ijhydene.2013.08.122>
64. N.T.Q. Nguyen and H.H. Yoon, *J. Power Sources*, **231**, 213 (2013); <https://doi.org/10.1016/j.jpowsour.2013.01.011>
65. B.H. Park and G.M. Choi, *Solid State Ion.*, **262**, 345 (2014); <https://doi.org/10.1016/j.ssi.2013.10.016>
66. S.J. Skinner, *Int. J. Inorg. Mater.*, **3**, 113 (2001); [https://doi.org/10.1016/S1466-6049\(01\)00004-6](https://doi.org/10.1016/S1466-6049(01)00004-6)
67. J. George K, V.V. Halali, S. C. G, V. Suvina, M. Sakar and R.G. Balakrishna, *Inorg. Chem. Front.*, **7**, 2702 (2020); <https://doi.org/10.1039/D0QI00306A>
68. N.F. Atta, A. Galal and A.R.M. El-Gohary, *Sens. Actuators B Chem.*, **327**, 128879 (2021); <https://doi.org/10.1016/j.snb.2020.128879>
69. J. He, J. Sunarso, Y. Zhu, Y. Zhong, J. Miao, W. Zhou and Z. Shao, *Sens. Actuators B Chem.*, **244**, 482 (2017); <https://doi.org/10.1016/j.snb.2017.01.012>
70. T.W. Chen, R. Ramachandran, S.M. Chen, N. Kavitha, K. Dinakaran, R. Kannan, G. Anushya, N. Bhuvana, T. Jeyapragasam, V. Mariyappan, S. Divya Rani and S. Chitra, *Catalysts*, **10**, 938 (2020); <https://doi.org/10.3390/catal10080938>
71. M.A. Mohamed, M.M. Hasan, I.H. Abdullah, A.M. Abdellah, A.M. Yehia, N. Ahmed, W. Abbas and N.K. Allam, *Talanta*, **185**, 344 (2018); <https://doi.org/10.1016/j.talanta.2018.03.104>
72. C. Sun, J.A. Alonso and J. Bian, *Adv. Energy Mater.*, (2020); <https://doi.org/10.1002/aenm.202000459>
73. A. Kostopoulou, K. Brintakis, N.K. Nasikas and E. Stratakis, *Nanophotonics*, **8**, 1607 (2019); <https://doi.org/10.1515/nanoph-2019-0119>
74. P. Ramasamy, D.-H. Lim, B. Kim, S.-H. Lee, M.-S. Lee and J.-S. Lee, *Chem. Commun.*, **52**, 2067 (2015); <https://doi.org/10.1039/C5CC08643D>
75. J. Zhu, H. Li, L. Zhong, P. Xiao, X. Xu, X. Yang, Z. Zhao, *ACS Catal.*, **4**, 2917 (2014); <https://doi.org/10.1021/cs500606g>
76. E.A.R. Assirey, *Saudi Pharm. J.*, **27**, 817 (2019); <https://doi.org/10.1016/j.jsps.2019.05.003>
77. T. Vijayaraghavan, R. Sivasubramanian, S. Hussain and A. Ashok, *ChemistrySelect*, **2**, 5570 (2017); <https://doi.org/10.1002/slct.201700723>
78. Y. Wang, L. Luo, Y. Ding, X. Zhang, Y. Xu and X. Liu, *J. Electroanal. Chem.*, **667**, 54 (2012); <https://doi.org/10.1016/j.jelechem.2011.12.021>
79. L. Zhu, R. Ran, M. Tade, W. Wang and Z. Shao, *Asia-Pac. J. Chem. Eng.*, **11**, 338 (2016); <https://doi.org/10.1002/apj.2000>
80. E.A. Katz, *Helv. Chim. Acta*, **103**, e2000061 (2020); <https://doi.org/10.1002/hlca.202000061>
81. P.C. Reshmi Varma, *Perovskite Photovoltaics*, 197 (2018); <https://doi.org/10.1016/B978-0-12-812915-9.00007-1>
82. C. Artini, *J. Eur. Ceram. Soc.*, **37**, 427 (2017); <https://doi.org/10.1016/j.jeurceramsoc.2016.08.041>
83. H. Zhang, N. Li, K. Li and D. Xue, *Acta Crystallogr.*, **63**, 812 (2007); <https://doi.org/10.1107/S0108768107046174>
84. S.F. Hoefler, G. Trimmel and T. Rath, *Monatsh. Chem.*, **148**, 795 (2017); <https://doi.org/10.1007/s00706-017-1933-9>
85. L. Wu, Z. Wang, B. Zhang, L. Yu, G.M. Chow, J. Tao, M.-G. Han, H. Guo, L. Chen, E.W. Plummer, J. Zhang and Y. Zhu, *Microsc. Microanal.*, **23(S1)**, 1586 (2017); <https://doi.org/10.1017/S1431927617008595>

86. Z. Song and Q. Liu, *Inorg. Chem. Front.*, **7**, 1583 (2020); <https://doi.org/10.1039/D0QI00016G>
87. C.N.R. Rao, Encyclopedia of Physical Science and Technology, 707 (2003); <https://doi.org/10.1016/B0-12-227410-5/00554-8>
88. L. Clark and P. Lightfoot, Eds. A. Tressaud and K. Poepplmeier, Photonic and Electronic Properties of Fluoride Materials: Progress in Fluorine Science Series, Progress in Fluorine Science, Elsevier, Ed.: 1, pp. 261-284 (2016); <https://doi.org/10.1016/B978-0-12-801639-8.00013-1>
89. S.K. Sahoo, B. Manoharan and N. Sivakumar, *Perovskite Photovoltaics*, 1 (2018); <https://doi.org/10.1016/B978-0-12-812915-9.00001-0>
90. C. L.C. Ellis, E. Smith, H. Javaid, G. Berns and D. Venkataraman, *Perovskite Photovoltaics*, 163 (2018); <https://doi.org/10.1016/B978-0-12-812915-9.00006-X>
91. M. Johansson and P. Lemmens, Crystallography and Chemistry of Perovskites, In: Handbook of Magnetism and Advanced Magnetic Materials, Wiley (2007).
92. C. Artini, *J. Eur. Ceram.*, **37**, 427 (2017); <https://doi.org/10.1016/j.jeurceramsoc.2016.08.041>
93. A. Navrotsky, *Chem. Mater.*, **10**, 2787 (1998); <https://doi.org/10.1021/cm9801901>
94. S.C. Watthage, Z. Song, A.B. Phillips and M. J. Heben, *Perovskite Photovoltaics*, Chap. 3, pp. 43-88 (2018); <https://doi.org/10.1016/B978-0-12-812915-9.00003-4>
95. K. Hirose, R. Wentzcovitch, D.A. Yuen and T. Lay, *Treatise on Geophysics*, **2**, 85 (2015); <https://doi.org/10.1016/B978-0-444-53802-4.00054-3>
96. T. Duffy, N. Madhusudhan and K.K.M. Lee, *Treatise on Geophysics*, **2**, 149 (2015); <https://doi.org/10.1016/B978-0-444-53802-4.00053-1>
97. M.W. Lufaso and P.M. Woodward, *Acta Crystallogr. B*, **60**, 10 (2004); <https://doi.org/10.1107/S0108768103026661>
98. G.B. Stracher, *Coal and Peat Fires: A Global Perspective*, **5**, 243 (2019); <https://doi.org/10.1016/B978-0-12-849885-9.00013-5>
99. C.H. Yan, Z.G. Yan, Y.P. Du, J. Shen, C. Zhang and W. Feng, Handbook on the Physics and Chemistry of Rare Earths, vol. 41, p. 275 (2011); <https://doi.org/10.1016/B978-0-444-53590-0.00004-2>
100. Y. Liu, Z. Yang and S. Liu, *Adv. Sci.*, **5**, 1700471 (2018); <https://doi.org/10.1002/advs.201700471>
101. H.U. Habermeier, *Mater. Today*, **10**, 34 (2007); [https://doi.org/10.1016/S1369-7021\(07\)70243-2](https://doi.org/10.1016/S1369-7021(07)70243-2)
102. T. Ye, X. Wang, X. Li, A.Q. Yan, S. Ramakrishna and J. Xu, *J. Mater. Chem. C Mater. Opt. Electron. Devices*, **5**, 1255 (2017); <https://doi.org/10.1039/C6TC04594D>
103. C.C. Stoumpos and M.G. Kanatzidis, *Adv. Sci.*, **28**, 5778 (2016); <https://doi.org/10.1002/adma.201600265>
104. J. Ding, Z. Lian, Y. Li, S. Wang and Q. Yan, *J. Phys. Chem. Lett.*, **9**, 4221 (2018); <https://doi.org/10.1021/acs.jpcclett.8b01898>
105. B. Murali, H.K. Kolli, J. Yin, R. Ketavath, O.M. Bakr and O.F. Mohammed, *ACS Mater. Lett.*, **2**, 184 (2020); <https://doi.org/10.1021/acsmaterialslett.9b00290>
106. M.A. Pena and L.G. Fierro, *Chem. Rev.*, **101**, 1981 (2001); <https://doi.org/10.1021/cr980129f>
107. M.I. Saidaminov, V. Adinolfi, R. Comin, A.L. Abdelhady, W. Peng, I. Dursun, M. Yuan, S. Hoogland, E.H. Sargent and O.M. Bakr, *Nat. Commun.*, **6**, 8724 (2015); <https://doi.org/10.1038/ncomms9724>
108. Y. Liu, Y. Zhang, Z. Yang, D. Yang, X. Ren, L. Pang and S. Liu, *Adv. Sci.*, **28**, 9204 (2016); <https://doi.org/10.1002/adma.201601995>
109. Y. Jiang, M.A. Green, R. Sheng and A. Ho-Baillie, *Sol. Energy Mater. Sol. Cells*, **137**, 253 (2015); <https://doi.org/10.1016/j.solmat.2015.02.017>
110. Y. Dang, D. Ju, L. Wang and X. Tao, *CrystEngComm*, **18**, 4476 (2016); <https://doi.org/10.1039/C6CE00655H>
111. T. Ye, W. Fu, J. Wu, Z. Yu, X. Jin, H. Chen and H. Li, *J. Mater. Chem. A Mater. Energy Sustain.*, **4**, 1214 (2016); <https://doi.org/10.1039/C5TA10155G>
112. J.N. Wilson, J.M. Frost, S.K. Wallace and A. Walsh, *APL Mater.*, **7**, 010901 (2019); <https://doi.org/10.1063/1.5079633>
113. W.J. Yin, Y. Yan and S.H. Wei, *J. Phys. Chem. Lett.*, **5**, 3625 (2014); <https://doi.org/10.1021/jz501896w>
114. R. Babu, L. Giribabu and S.P. Singh, *Cryst. Growth Des.*, **18**, 2645 (2018); <https://doi.org/10.1021/acs.cgd.7b01767>
115. D.N. Dirin, I. Cherniukh, S. Yakunin, Y. Shynkarenko and M.V. Kovalenko, *Chem. Mater.*, **28**, 8470 (2016); <https://doi.org/10.1021/acs.chemmater.6b04298>
116. S.K. Sahoo, B. Manoharan and N. Sivakumar, Introduction: Why Perovskite and Perovskite Solar Cells? In: Perovskite Photovoltaics, Basic to Advanced Concepts and Implementation, Academic Press, Chap. 1, pp. 1-24 (2018).
117. C. Zuo and L. Ding, *Angew. Chem. Int. Ed.*, **56**, 6528 (2017); <https://doi.org/10.1002/anie.201702265>
118. Z. Fan, K. Sun and J. Wang, *J. Mater. Chem. A Mater. Energy Sustain.*, **3**, 18809 (2015); <https://doi.org/10.1039/C5TA04235F>
119. S. Yakunin, M. Sytnyk, D. Kriegner, S. Shrestha, M. Richter, G.J. Matt, H. Azimi, C.J. Brabec, J. Stangl, M.V. Kovalenko and W. Heiss, *Nat. Photonics*, **9**, 444 (2015); <https://doi.org/10.1038/nphoton.2015.82>
120. J. Ding and Q. Yan, *Sci. China Mater.*, **60**, 1063 (2017); <https://doi.org/10.1007/s40843-017-9039-8>
121. I. Choi, S.J. Lee, J.C. Kim, Y.-G. Kim, D.-Y. Hyeon, K.S. Hong, J. Suh, D. Shin, H.Y. Jeong and K.I. Park, *Appl. Surf. Sci.*, **511**, 145614 (2020); <https://doi.org/10.1016/j.apsusc.2020.145614>
122. Y. Huang, Y. Feng, F. Li, F. Lin, Y. Wang, X. Chen and R. Xie, *TrAC Trends Analyt. Chem.*, **134**, 116127 (2020); <https://doi.org/10.1016/j.trac.2020.116127>
123. J. Wolanyk, X. Xiao, M. Fralalde, N.J. Lauersdorf, R. Kaudal, E. Dykstra, J. Huang, J. Shinar and R. Shinar, *Sens. Actuators B Chem.*, **321**, 128462 (2020); <https://doi.org/10.1016/j.snb.2020.128462>
124. F. Rahimi, A.K. Jafari, C.A. Hsu, C.S. Ferekides and A.M. Hoff, *Org. Electron.*, **75**, 105397 (2019); <https://doi.org/10.1016/j.orgel.2019.105397>
125. P. Kaur and K. Singh, *Ceram. Int.*, **46**, 5521 (2020); <https://doi.org/10.1016/j.ceramint.2019.11.066>
126. K. Wang, C. Han, Z. Shao, J. Qiu, S. Wang and S. Liu, *Adv. Funct. Mater.*, **31**, 30 (2021); <https://doi.org/10.1002/adfm.202102089>
127. M. Misono, *Stud. Surf. Sci. Catal.*, **176**, 67 (2013); <https://doi.org/10.1016/B978-0-444-53833-8.00003-X>
128. J.L. Hueso, A. Caballero, J. Cotrino and A.R. González-Elipe, *Catal. Commun.*, **8**, 1739 (2007); <https://doi.org/10.1016/j.catcom.2007.02.001>
129. B. Mohanty, S. Bhattacharjee, R.K. Parida and B.N. Parida, *Mater. Today Proc.*, **35**, 91 (2021); <https://doi.org/10.1016/j.matpr.2020.03.068>
130. J. Lu, Y. Li and Y. Ding, *Ceram. Int.*, **46**, 7741 (2020); <https://doi.org/10.1016/j.ceramint.2019.11.277>
131. D. Yang, W. Zhang, Y. Wang, L. Li, F. Yao, L. Miao, W. Zhao, X. Kong, Q. Feng and D. Hu, *Ceram. Int.*, **47**, 1479 (2021); <https://doi.org/10.1016/j.ceramint.2020.08.274>
132. S. Tasleem and M. Tahir, *Int. J. Hydrog. Energy*, **45**, 19078 (2020); <https://doi.org/10.1016/j.ijhydene.2020.05.090>
133. S. Bhattacharjee, B. Mohanty, N.C. Nayak, R.K. Parida and B.N. Parida, *Mater. Sci. Semicond. Process.*, **123**, 105503 (2021); <https://doi.org/10.1016/j.mssp.2020.105503>
134. S. Jiang, T. Hu, J. Gild, N. Zhou, J. Nie, M. Qin, T. Harrington, K. Vecchio and J. Luo, *Scr. Mater.*, **142**, 116 (2018); <https://doi.org/10.1016/j.scriptamat.2017.08.040>
135. H. Wang, M. Zhou, P. Choudhury and H. Luo, *Appl. Mater. Today*, **16**, 56 (2019); <https://doi.org/10.1016/j.apmt.2019.05.004>
136. S. Arya, P. Mahajan, R. Gupta, R. Srivastava, N.K. Tailor, S. Satapathi, R. Sumathi, R. Datt and V. Gupta, *Prog. Solid State Chem.*, **60**, 100286 (2020); <https://doi.org/10.1016/j.progsolidchem.2020.100286>

137. L. Zhang, J. Miao, J. Li and Q. Li, *Adv. Funct. Mater.*, **30**, 2003653 (2020); <https://doi.org/10.1002/adfm.202003653>
138. L. He, Y. Shu, W. Li and M. Liu, *J. Mater. Sci. Mater. Electron.*, **30**, 17 (2019); <https://doi.org/10.1007/s10854-018-0331-3>
139. H. Mo, H. Nan, X. Lang, S. Liu, L. Qiao, X. Hu and H. Tian, *Ceram. Int.*, **44**, 9733 (2018); <https://doi.org/10.1016/j.ceramint.2018.02.205>
140. M.A. Bavio, J.E. Tasca, G.G. Acosta, M.F. Ponce, R.O. Fuentes and A. Visintin, *J. Solid State Chem.*, **24**, 699 (2020); <https://doi.org/10.1007/s10008-020-04511-7>
141. K.H. Ho and J. Wang, *J. Am. Ceram. Soc.*, **100**, 4629 (2017); <https://doi.org/10.1111/jace.14997>
142. T.N. Vinuth Raj, P.A. Hoskeri, H.B. Muralidhara, C.R. Manjunatha, K. Yogesh Kumar and M.S. Raghu, *J. Electroanal. Chem.*, **858**, 113830 (2020); <https://doi.org/10.1016/j.jelechem.2020.113830>
143. Z. Xu, Y. Liu, W. Zhou, M.O. Tade and Z. Shao, *ACS Appl. Mater. Interfaces*, **10**, 9415 (2018); <https://doi.org/10.1021/acsaami.7b19391>
144. C.H. Ng, H.N. Lim, S. Hayase, Z. Zainal, S. Shafie, H.W. Lee and N.M. Huang, *ACS Appl. Energy Mater.*, **1**, 692 (2018); <https://doi.org/10.1021/acsaem.7b00103>
145. A. Slonopas, H. Ryan and P. Norris, *Electrochim. Acta*, **307**, 334 (2019); <https://doi.org/10.1016/j.electacta.2019.03.221>
146. L.E. Oloore, M.A. Gondal, I.K. Popoola and A. Popoola, *ChemElectroChem*, **7**, 486 (2020); <https://doi.org/10.1002/celec.201901969>
147. P. Maji, A. Ray, P. Sadhukhan, A. Roy and S. Das, *Mater. Lett.*, **227**, 268 (2018); <https://doi.org/10.1016/j.matlet.2018.05.101>
148. L.E. Oloore, M.A. Gondal, A. Popoola and I.K. Popoola, *Electrochim. Acta*, **361**, 137082 (2020); <https://doi.org/10.1016/j.electacta.2020.137082>
149. P. Andriëvic, X. Mettan, M. Kollár, B. Náfrádi, A. Sienkiewicz, T. Garma, L. Rossi, L. Forró and E. Horváth, *ACS Photonics*, **6**, 967 (2019); <https://doi.org/10.1021/acsp Photonics.8b01653>
150. J. Hao, W. Li, J. Zhai and H. Chen, *Mater. Sci. Eng. Rep.*, **135**, 1 (2019); <https://doi.org/10.1016/j.mseri.2018.08.001>
151. Y. Masubuchi, S.K. Sun and S. Kikkawa, *Dalton Trans.*, **44**, 10570 (2015); <https://doi.org/10.1039/C4DT03811H>
152. Y.X. Gan, A.H. Jayatissa, Z. Yu, X. Chen and M. Li, *J. Nanomater.*, **2020**, 8917013 (2020); <https://doi.org/10.1155/2020/8917013>
153. S. Somya and R. Roy, *Bull. Mater. Sci.*, **23**, 453 (2000); <https://doi.org/10.1007/BF02903883>
154. H.Y. Kim, J. Shin, I.C. Jang and Y.W. Ju, *Energies*, **13**, 36 (2019); <https://doi.org/10.3390/en13010036>
155. A. Rezanezhad, E. Rezaie, L.S. Ghadimi, A. Hajalilou, E. Abouzari-Lotf and N. Arsalani, *Electrochim. Acta*, **335**, 135699 (2020); <https://doi.org/10.1016/j.electacta.2020.135699>
156. J. Singh, A. Kumar, U.K. Goutam and A. Kumar, *Appl. Phys., A Mater. Sci. Process.*, **126**, 11 (2020); <https://doi.org/10.1007/s00339-019-3195-3>
157. S. Nagamuthu, S. Vijayakumar and K.S. Ryu, *Mater. Chem. Phys.*, **199**, 543 (2017); <https://doi.org/10.1016/j.matchemphys.2017.07.050>
158. M. Rafique, S. Hajra, M.Z. Iqbal, G. Nabi, S.S.A. Gillani and M. Bilal Tahir, *Int. J. Energy Res.*, **45**, 4145 (2021); <https://doi.org/10.1002/er.6075>
159. H. Wang, Q. Luo, M. Sun, X. Yin and L. Wang, *J. Mater. Chem. C Mater. Opt. Electron. Devices*, **8**, 12355 (2020); <https://doi.org/10.1039/D0TC02354J>
160. A.S. Paluch, S. Jayaraman, J.K. Shah and E.J. Maginn, *J. Chem. Phys.*, **133**, 124504 (2010); <https://doi.org/10.1063/1.3478539>
161. M.P. Harikrishnan and A.C. Bose, *AIP Conf. Proc.*, **2115**, 030129 (2019); <https://doi.org/10.1063/1.5112968>
162. W. Mi, C. Dai, S. Zhou, J. Yang, Q. Li and Q. Xu, *Mater. Lett.*, **227**, 66 (2018); <https://doi.org/10.1016/j.matlet.2018.04.131>
163. K.P. Cheng, R.J. Gu and L.X. Wen, *RSC Adv.*, **10**, 11681 (2020); <https://doi.org/10.1039/D0RA01411G>
164. M.P. Harikrishnan and A.C. Bose, *AIP Conf. Proc.*, **2082**, 060001 (2019); <https://doi.org/10.1063/1.5093874>
165. P. Lannelongue, S. Le Vot, O. Fontaine, T. Brousse and F. Favier, *Electrochim. Acta*, **326**, 134886 (2019); <https://doi.org/10.1016/j.electacta.2019.134886>
166. M.P. Harikrishnan and A.C. Bose, *AIP Conf. Proc.*, **2265**, 030631 (2020); <https://doi.org/10.1063/5.0016695>
167. R. Sui and P. Charpentier, *Chem. Rev.*, **112**, 3057 (2012); <https://doi.org/10.1021/cr2000465>
168. Z.A. Elsiddig, H. Xu, D. Wang, W. Zhang, X. Guo, Y. Zhang, Z. Sun and J. Chen, *Electrochim. Acta*, **253**, 422 (2017); <https://doi.org/10.1016/j.electacta.2017.09.076>
169. A.K. Tomar, G. Singh and R.K. Sharma, *ChemSusChem*, **11**, 4123 (2018); <https://doi.org/10.1002/cssc.201801869>
170. G. George, S.L. Jackson, C.Q. Luo, D. Fang, D. Luo, D. Hu, J. Wen and Z. Luo, *Ceram. Int.*, **44**, 21982 (2018); <https://doi.org/10.1016/j.ceramint.2018.08.313>
171. A.K. Tomar, G. Singh and R.K. Sharma, *J. Power Sources*, **426**, 223 (2019); <https://doi.org/10.1016/j.jpowsour.2019.04.049>
172. N. Kitchamsetti, R.J. Choudhary, D.M. Phase and R.S. Devan, *RSC Adv.*, **10**, 23446 (2020); <https://doi.org/10.1039/D0RA04052E>
173. N. Kitchamsetti, Y.R. Ma, P.M. Shirage and R.S. Devan, *J. Alloys Compd.*, **833**, 155134 (2020); <https://doi.org/10.1016/j.jallcom.2020.155134>
174. A.V. Nikam, B.L.V. Prasad and A.A. Kulkarni, *CrystEngComm*, **20**, 5091 (2018); <https://doi.org/10.1039/C8CE00487K>
175. Y.B. Pottathara, Y. Grohens, V. Kokol, N. Kalarikkal and S. Thomas, *Nanomater. Synth.*, **1-25** (2019); <https://doi.org/10.1016/B978-0-12-815751-0.00001-8>
176. A. Kumar and A. Kumar, *Ceram. Int.*, **45**, 14105 (2019); <https://doi.org/10.1016/j.ceramint.2019.04.110>
177. N.F. Mansoorie, J. Singh and A. Kumar, *Mater. Sci. Semicond. Process.*, **107**, 104826 (2020); <https://doi.org/10.1016/j.mssp.2019.104826>
178. M. Ickler, M. Devi, I. Rogge, J. Singh and A. Kumar, *J. Mater. Sci. Mater. Electron.*, **31**, 6977 (2020); <https://doi.org/10.1007/s10854-020-03263-4>
179. A. Kumar, A. Kumar and A. Kumar, *Solid State Sci.*, **105**, 106252 (2020); <https://doi.org/10.1016/j.solidstatesciences.2020.106252>
180. J. Singh and A. Kumar, *Mater. Sci. Semicond. Process.*, **99**, 8 (2019); <https://doi.org/10.1016/j.mssp.2019.04.007>
181. P. Palanisamy, K. Thangavel, S. Murugesan, S. Marappan, M. Chavali, P.F. Siril and D.V. Perumal, *J. Electroanal. Chem.*, **833**, 93 (2019); <https://doi.org/10.1016/j.jelechem.2018.11.026>